Emergo
Studies in the Biogeophysical Environment

Tillage effects on pesticide losses to drains in a heavy clay soil at Lanna, Sweden: Measurements and modelling

[1]Mats Larsbo, [2]Mark Greener and [1]Nicholas Jarvis

[1]Department of Soil Sciences, SLU, Box 7014, 750 07 Uppsala, Sweden

[2]Syngenta Limited, Priestley Road, Surrey Research Park, Guilford, Surrey GU2 7YH, United Kingdom

Swedish University of Agricultural Sciences	Emergo 2007:2
Department of Soil Sciences	Report
Division of Environmental Physics	ISSN 1651-7210
	ISBN 978-91-85911-25-7

ABSTRACT

Soil tillage effects are not accounted for in the surface water pesticide leaching scenarios used within the EU for regulatory modelling even though tillage has been shown to influence pesticide leaching. The objectives of this study were, (i) to evaluate differences between conventional (*C*) and no-till (*NT*) systems in water flow and solute transport in the topsoil of a heavy clay soil prone to preferential flow, (ii) to calibrate key model parameters governing preferential flow in the dual-permeability model MACRO 5.1 from laboratory microlysimeter measurements, and (iii) to study differences in pesticide leaching in simulations based on the FOCUS surface water D1 scenario and calibrated parameter values for *C* and *NT*. Both *C* and *NT* microlysimeters exhibited strong preferential flow. The breakthrough was generally faster for the *NT* microlysimeters, but the variability within treatments was large. Five parameters, the parameter governing mass exchange between pore domains in two soil horizons, the kinematic exponent in the macropores, the macroporosity and the initial water content were included in the calibration. The observed differences in water flow and chloride leaching between treatments were reflected in the values for the parameter governing mass exchange between pore domains in the surface 6 cm of soil and in the macroporosity. Mass exchange was weaker and macroporosity was smaller in the *NT* soil, both of which promote faster non-equilibrium macropore flow and transport. The differences in the scenario simulations between *C* and *NT* were small for drainage rates. For a weakly sorbed easily degraded compound and a strongly sorbed slowly degraded compound, the scenario simulations predicted 3.4 and 4.6 times larger average concentrations in drainage water respectively for *NT* compared with *C*. The maximum hourly concentrations in drainage water using best parameter estimates were 3.4 and 12 times larger for *NT* compared with *C* for the same compounds. The uncertainties in the concentrations in drainage water were large. This uncertainty reflects spatial variability in the field, errors in parameter values not included in the calibration, parameter correlations and model error. More data and refined methods to better account for the spatial variability are needed in future research to reduce the uncertainty in predictions of tillage effects in regulatory modelling.

CONTENTS

INTRODUCTION

Soil tillage has been shown to influence pesticide leaching both at the field scale (Isensee et al., 1990) and in lysimeter experiments (Brown et al., 1999a). However, tillage effects are not included in pesticide leaching models used within the EU for registration of new compounds probably because of the large amount of data needed for parameterisation. Including tillage effects in the EU pre-defined scenarios for pesticide leaching to groundwater and surface waters might lead to more reliable estimates of pesticide concentrations, and possibilities to identify 'best management practices' that minimize leaching losses.

Tillage alters the pore geometry of the topsoil creating favourable conditions for plant root growth. These changes influence the hydraulic properties of the soil and also the water flow and solute transport pathways. Tillage mainly alters the large pore classes leaving the intra-aggregate pores unaltered (Mapa et al., 1986). Tillage has the potential to limit macropore flow by disrupting macropore continuity (Meek et al., 1990), both at plough depth and the depth of secondary tillage (e.g. harrowing). Changes induced by tillage are slowly reversed over time by natural processes such as wetting/drying and freezing/thawing and by consolidation due to traffic (Mapa et al., 1986). The changes in hydraulic properties can lead to temporal changes in water flow and solute transport (Dunn and Philips, 1991).

Reduced tillage (*RT*) or no-till (*NT*) systems have been implemented to reduce soil erosion or to reduce production costs. However, these practices may also have effects on pesticide leaching. Conventional tillage (*C*) is generally considered to reduce pesticide leaching (Isensee et al., 1990; Elliot et al., 2000) in soils where preferential flow and transport is significant by cutting continuous macropores that act as preferential flow paths in *RT* and *NT* soils (Edwards et al., 1988). A larger fraction of continuous macropores in *NT* soils has also been shown through the use of staining techniques (Heard et al., 1988). In soils where preferential flow is of minor importance, *C* has been reported to increase pesticide leaching (Gish et al., 1995; Sadeghi et al., 1998) or have insignificant effects (Gaynor et al., 1995). The likely reason for the smaller leaching in *RT* and *NT* in such cases is the higher organic matter content (and microbial activity) in the topsoil, which increases sorption and degradation of pesticides.

For a model to be useful in an evaluation of tillage effects on pesticide leaching, the model must account for the effects tillage exerts on the soil structure and macropore geometry. One such model is MACRO 5.1 (Larsbo et al., 2005). The MACRO model has been widely used in research and in regulatory modelling both in Sweden and within the EU, but so far the effects of tillage have been neglected due to lack of information on how to parameterise these processes. Few attempts have been made to translate the effects of tillage on water flow and transport into model parameters (Brown et al., 1999b) and to our knowledge no attempts have been made using replicated data from lysimeter studies.

The objectives of this study were, (i) to evaluate temporal changes and differences between *C* and *NT* systems in soil physical and hydraulic properties, water flow and solute transport in the topsoil of a heavy clay soil, prone to preferential flow, (ii) to calibrate key model parameters governing preferential flow in the dual-permeability model MACRO 5.1 from laboratory microlysimeter measurements, and (iii) to study differences in pesticide leaching in long-term simulations based on the FOCUS D1 surface water scenario (FOCUS, 2001) and calibrated parameter values for *C* and *NT*.

The process to achieve these objectives consisted of three main parts:

1. *Microlysimeter experiments*: Water flow and solute transport were studied in microlysimeters sampled during one growing season on *C* and *NT* fields.
2. *Calibration*: Measurements from the microlysimeter experiments were used to calibrate important model parameters using the GLUE (generalised likelihood uncertainty estimation) method.
3. *Scenario simulations*: The parameter values attained in the calibration were used in two sets of scenario simulations, (i) GLUE scenario simulations, taking uncertainty into account, and (ii) deterministic scenario simulations, using best estimate parameter values for *C* and *NT*.

LABORATORY EXPERIMENTS

Material and methods

The field site

Lanna, Sweden (lat. 58°21', long. 13°08') is one of six sites included in the FOCUS surface water scenarios (FOCUS, 2001) for pesticide losses via drains. The soil is a well-structured silty clay, classified by Bergström et al. (1994) as a Typic Eutrochrept (USDA). Larsson and Jarvis (1999) reported a high degree of preferential flow and solute transport for the Lanna soil. Lanna is situated on a flat plain, with the slope at the field site less than 1%. The location of the field site is shown in fig. 1. Microlysimeters (18 cm high, 20 cm diameter undisturbed soil columns enclosed in PVC plastic pipes) and small cylinders (5 cm high, 7 cm diameter) were taken at two locations, one conventionally tilled (*C*) (autumn mouldboard ploughing to a depth of ca. 25 cm, harrowing on 12 April to a depth of ca. 6 cm) field with spring-sown oats (*Avena Sativa* L.) and one field, which had been under no-till without straw incorporation (*NT*) for 23 years directly sown with winter wheat (*Triticum Vulgare* L.) the preceding autumn.

Sampling

The sampling scheme is summarised in Table 1. Four replicate microlysimeters were taken from the *C* field on four occasions and from the *NT* field on three occasions during the growing season of 2005. The first sampling was on 8 April (*pre-spring sowing*), the second (only *C*) on 3 May (*early growing season*), the third on 15 June (*mid growing season*) and the fourth on 15 August (*pre-harvest*). Three replicate cylinders (5 cm in height, 7 cm in diameter) were taken close to the microlysimeters at each sampling. The samples were stored until the start of the laboratory experiments at 2°C to minimize biological activity. All microlysimeters were taken from the soil surface, whereas the small cylinders were taken 2 cm below the soil surface. The small cylinders were used for measurements of bulk density and soil water content at the pressure heads -2.5, -20, -50, -100 and -600 cm. Soil water contents at the pressure heads -5000 and -15000 cm were measured for three samples from each of the fields since these measurements are dependent on the particle size distribution only and should not be expected to vary over time. The van Genuchten equation (van Genuchten, 1980) was fitted to the water retention data for each individual cylinder using the RETC program (van Genuchten et al., 1991). Only measurements smaller than -0.2 m pressure head were used for the curve fitting since pressure heads corresponding to the macropore region should not influence the water retention function for the micropores. Measurements of total carbon content were made on samples from 3 and 10 cm depths and particle size distribution on samples from 10 cm depth for both fields.

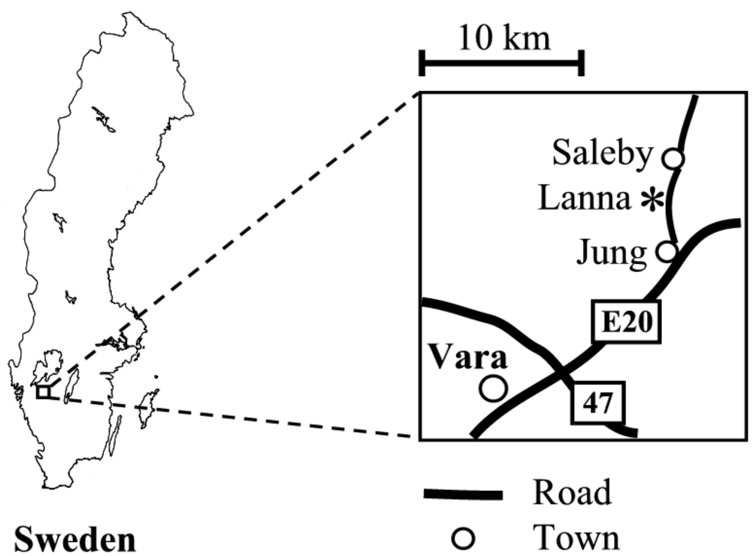

Fig. 1. Location map of Lanna.

Table 1. Field sampling scheme.

Designate	Date	Nr. of microlysimeters		Nr. of small cylinders	
		C	*NT*	*C*	*NT*
Pre-spring sowing	8 April	4	4	3	3
Early growing season	3 May	4	-	3	-
Mid-growing season	15 June	4	4	3	3
Pre-harvest	15 August	4	4	3	3

Microlysimeter experiments

The microlysimeters were installed in the laboratory allowing free drainage through plastic filters. Irrigation was supplied from air-atomising nozzles located 1.2 m above each microlysimeter. The nozzles create a fine mist with low kinetic energy, minimising the impact at the soil surface thus retaining the soil structure throughout the experiment. The microlysimeters were irrigated four times with filtered rainwater (chloride concentration < 0.5 mg dm^{-3}) at intensities varying between 10 and 16 mm h^{-1} (Table 2). The first irrigation lasted one hour and the following three lasted 40 minutes followed by a 5 minute break and 15 more minutes of irrigation. The irrigations were carried out at 1 pm on day 1, 5, 8 and 11 from the start of the experiment. Before the second irrigation, at 1 pm on day 4, 25 ml of KCl solution with a concentration of 20 g Cl dm^{-3} (= dose of 16.9 g m^{-2}) was applied to each microlysimeter using a hand-held air-atomising sprayer. The drainage from the microlysimeters was collected in bottles and recorded 40, 60, 90, 180 and 4320 minutes after the start of each irrigation. Chloride concentrations in the percolated water were analysed using ion chromatography. After finishing the chloride transport experiments, infiltration rates were measured with a tension infiltrometer placed on top of each microlysimeter at the pressure heads -1, -3, -5 and -10 cm starting at -10 cm. All infiltration measurements were made at steady state flow. The diameter of the infiltration disc was the same as the diameter of the microlysimeters. A layer of moist fine sand was placed on the soil surface to get a good contact between the soil and the infiltrometer tension plate and to even out irregularities at the soil surface. For some microlysimeters, more than 1.5 cm sand was needed to achieve a horizontal surface. The thickness of the sand layer was accounted for when regulating the pressure head at the soil surface (Reynolds and Zebchuk, 1996).

Table 2. Irrigation rates for the laboratory microlysimeter experiment.

	Conventional tillage		No tillage	
	Nr	Irrigation rate (mm h^{-1})	Nr	Irrigation rate (mm h^{-1})
Pre-spring sowing	13	14.2	17	12.8
	14	14.7	18	13.8
	15	12.4	19	11.1
	16	10.4	20	12.9
Mid growing season	1	11.0	5	13.1
	2	-	6	15.6
	3	12.6	7	13.8
	4	11.1	8	-
Pre-harvest	21	-	25	13.0
	22	11.6	26	12.5
	23	-	27	10.7
	24	-	28	-
Average		12.3		12.9

Results and discussion

Soil properties

Particle size distributions for the *C* and *NT* fields are presented in Table 3. The differences between the fields are small which means that any possible differences between treatments in hydraulic properties, water flow and solute transport will be a consequence of different management practices. The total organic carbon contents for the *NT* field were 3.0 and 1.8% for the 0–6 cm depth and the 6–18 cm depth respectively. Due to the efficient mixing of plant residues at ploughing, the total organic carbon content was 1.7% in both topsoil horizons for the *C* samples. From a visual inspection of the microlysimeter bottoms, the occurrence of macropores (predominantly earthworm channels) with a radius larger than 1 mm was higher for *NT* compared to *C*.

Table 3. Particle size distribution (%) measured on samples from 10 cm depth.

Sample	Conventional tillage			No tillage		
	Clay (<2 μm)	Silt (2–60 μm)	Sand (>60 μm)	Clay (<2 μm)	Silt (2–60 μm)	Sand (>60 μm)
Pre-spring sowing	47.3	44.2	8.5	42.6	40.6	16.9†
Early growing season	45.9	44.6	9.6	-	-	-
Mid growing season	45.0	44.2	10.8	45.2	45.5	9.5
Pre-harvest	46.3	46.1	7.6			
Average	**46.1**	**44.4**	**9.5**	**43.8**	**43.1**	**13.2**

† 8% gravel (i.e. some stones in the sample)

Water retention measurements

The results from the water retention measurements and curve fitting using the RetC software are presented in Table A1.1 and A1.2. The fitted values of the van Genuchten water retention function are similar for all sampling occasions and both the *C* and *NT* treatments. The macroporosity, here defined as the difference in water content at the pressure head –2.5 cm and -20 cm, was much larger for the *pre-spring sowing* samples compared to all other samples (Table A1.1 and A1.2). Note that the estimated water contents at –2.5 cm at *pre-harvest* in the *C* plots are larger than the pore volume calculated from the measured bulk density, due to swelling of the samples during the laboratory experiment.

Infiltration measurements

The results from the tension infiltrometer measurements on the microlysimeters are presented in Table 4. Infiltration rates at -10 cm pressure head were similar for all sampling periods for both *C* and *NT*. For all other pressure heads, *C* generally had higher infiltration rates than *NT* indicating that the corresponding pore classes are more prevalent for *C*. This does not necessarily mean that the saturated hydraulic conductivity is larger for the *C* microlysimeters, since the largest pore fraction does not contribute to the flow at these pressure heads. For *C*, infiltration rates for the *pre-spring sowing* were smaller compared to *mid growing season* but the number of samples is small and within sample variation is large.

Table 4. Tension infiltrometer measurements made on each microlysimeter at the pressure heads -1, -3, -5 and -10 cm.

	Conventional tillage Infiltration rate (mm h^{-1})					No tillage Infiltration rate (mm h^{-1})				
Sampling	Nr	-1 cm	-3 cm	-5 cm	-10 cm	Nr	-1 cm	-3 cm	-5 cm	-10 cm
Pre-spring	13	25	3.4	1.2	0.12	17	2.8	1.0	0.29	0.058
sowing	14	55	6.2	0.81	0.14	18	15	0.58	0.23	0.12
	15	35	2.8	1.3	0.029	19	3.5	1.3	0.23	0.12
	16	71	6.6	0.81	0.17	20	36	1.6	0.40	0.12
Mid	1	-	1.4	0.35	-	5	-	-	-	-
growing	2	-	-	-	-	6	5.1	0.52	0.26	0.20
season	3	16	1.6	0.23	0.086	7	17	1.4	0.46	0.23
	4	13	1.0	0.46	0.17	8	-	-	-	-
Pre-	21	-	-	-	-	25	6.2	0.46	0.19	0.058
harvest	22	-	4.8	0.46	0.12	26	12	0.86	0.23	0.12
	23	-	-	-	-	27	9.2	0.86	0.17	0.12
	24	-	-	-	-	28	-	-	-	-
Average		36	3.5	0.69	0.12		12	0.95	0.27	0.12
St. Dev.		23	2.5	0.38	0.051		10	0.39	0.097	0.058

Water flow and chloride transport experiments

Due to surface ponding, eight of the *C* and two of the *NT* microlysimeters were removed from the experiment. These microlysimeters included all four from the *early growing season* sampling. The reduced number of microlysimeters available for analyses unfortunately limits the possibilities to study temporal trends in water flow and solute transport. The results from the microlysimeter experiments are presented in fig. 2 for the *C* microlysimeters and in fig. 3 for the *NT* microlysimeters. For *C*, the accumulated percolation varied between 0.17 and 0.38 pore volumes. The same numbers for *NT* were 0.15 and 0.42. The accumulated irrigation was between 0.45 and 0.67. The large variation in accumulated percolation cannot solely be explained by differences in irrigation intensities (Table 2). It seems likely that the initial water content also differed between microlysimeters. The accumulated leaching for *C* varied between 26 and 48% of the applied amount whereas the numbers for *NT* were 11 and 59%. There is also a large variation in the leaching pattern for individual microlysimeters in both *C* and *NT* treatments (fig. 3a and b), which is probably a consequence of the large variability in infiltration rates (Table 4) and macroporosity (Table A1.1 and A1.2). Solute leaching starts before the start of the third irrigation for all microlysimeters, which is an indication of strong preferential flow for both treatments. The breakthrough was generally faster for the *NT* microlysimeters, but the variability was large.

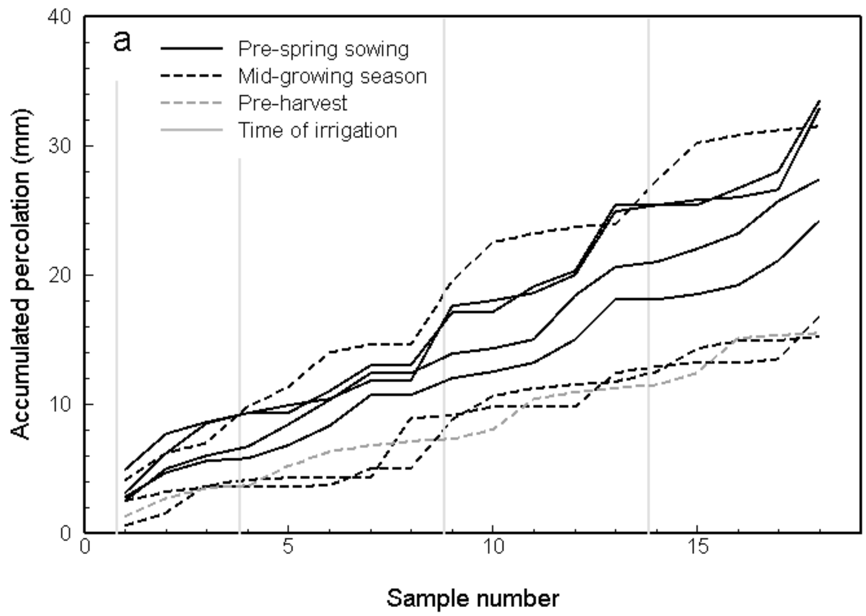

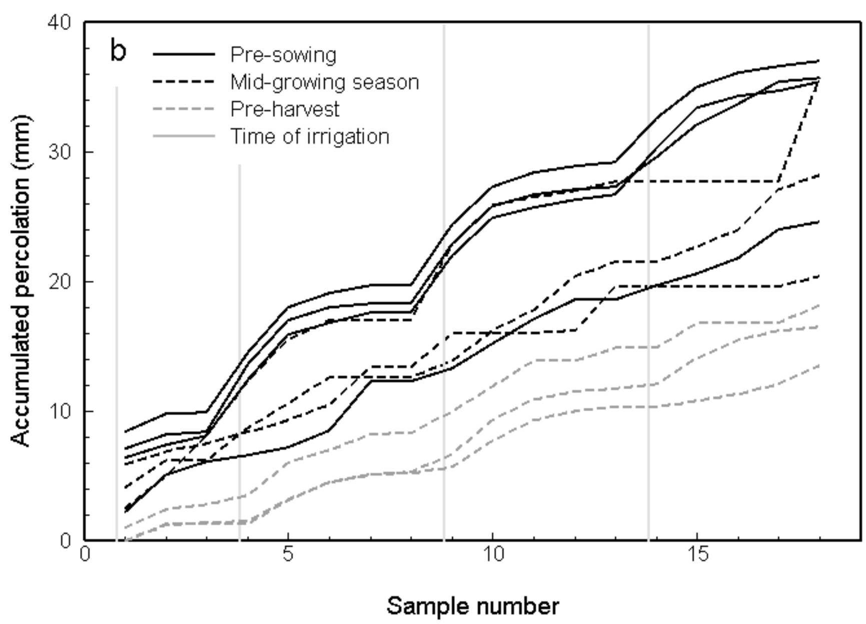

Fig 2. Measured accumulated percolation from all microlysimeters at the four sampling occasions, a) conventional tillage, and b) no tillage.

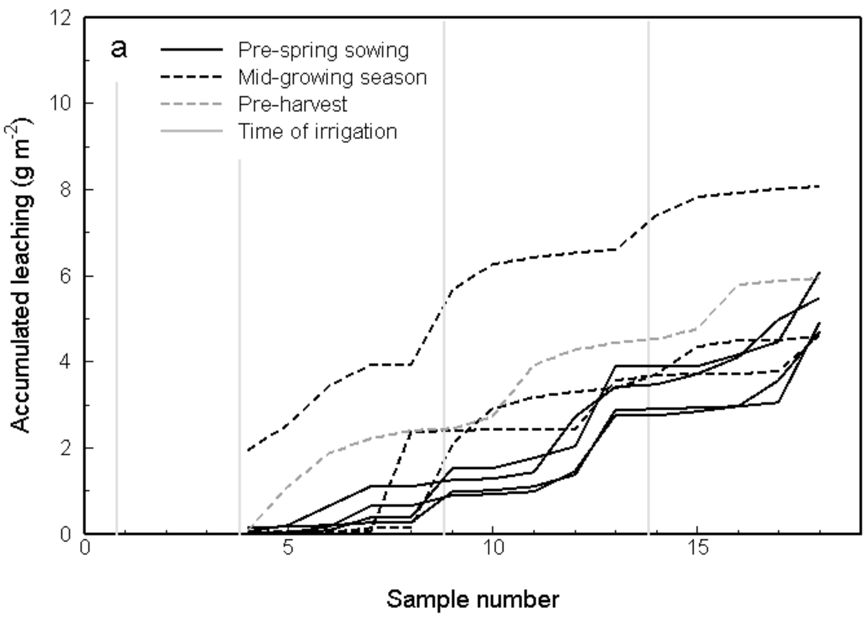

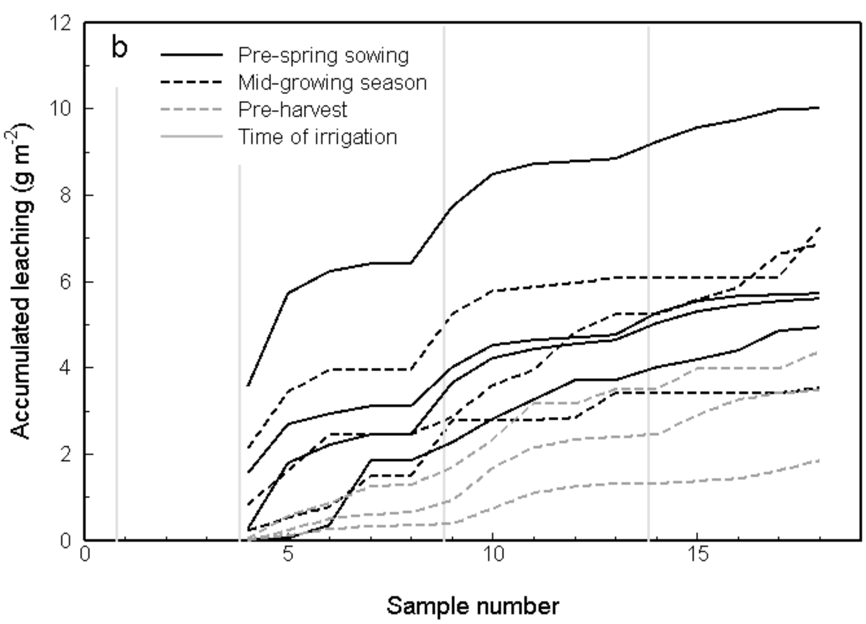

Fig 3. Measured accumulated leaching from all microlysimeters at the four sampling occasions, a) conventional tillage, and b) no tillage.

MODELLING

Model description

MACRO 5.1 is a physically based one-dimensional dual-permeability model for water flow and solute transport through the unsaturated zone (Larsbo and Jarvis, 2003; Larsbo et al., 2005). The soil porosity is divided into a micropore domain and a macropore domain. The pore domains are characterized by different flow rates and solute concentrations. Only the most relevant aspects of the model concerning this study are given here.

The division between flow domains is given by a water potential, ψ_b (m), and the corresponding saturated micropore water content, θ_b (-), and hydraulic conductivity, K_b (m s^{-1}), in the micropores. Water flow in the micropores is governed by Richards' equation:

$$C \frac{\partial \psi}{\partial t} = \frac{\partial}{\partial z}\left(K \left(\frac{\partial \psi}{\partial z} + 1 \right) \right) \pm S_w \qquad [1]$$

where $C = \partial\theta_{mic} / \partial\psi$ (m^{-1}) is the differential water capacity, θ_{mic} (-) is the volumetric micropore water content, ψ (m) is the soil water pressure head, t (s) is time, z (m) is the vertical coordinate (positive upwards), K (m s^{-1}) is the unsaturated micropore hydraulic conductivity, and S_w (s^{-1}) is a source-sink term accounting for water exchange with macropores. In the micropores, the water retention curve $\psi(\theta_{mic})$ is given by the van Genuchten (1980) function whereas the hydraulic conductivity function $K(\theta_{mic})$ is given by Mualem's (1976) model. Water flow in the macropores, q_{mac} (m s^{-1}) is described by a modified kinematic wave approach (Germann, 1985), where the macropores are assumed to drain by gravity only. The hydraulic conductivity in the macropores, K_{mac} (m s^{-1}), is expressed as a power function of the macropore water content, θ_{mac} (-):

$$q_{mac} = K_{mac} = K_{mac,sat} \left(\frac{\theta_{mac}}{\theta_{mac,sat}} \right)^{n^*} \qquad [2]$$

where $K_{mac,sat}$ (m s^{-1}) is the saturated conductivity of the macropores, $\theta_{mac,sat}$ (-) is the saturated macropore water content and n^* (-) is a 'kinematic' exponent reflecting macropore size distribution and tortuosity.

Lateral water flow from macropores to micropores is described as a first-order approximation to the water diffusion equation:

$$S_w = \left(\frac{G_f \; D_w \gamma_w}{d^2} \right) (\theta_b - \theta_{mic}) \qquad [3]$$

where d (m) is an effective diffusion pathlength related to aggregate size, D_w ($m^2\ s^{-1}$) is an effective water diffusivity, γ_w (-) is a scaling factor introduced to match the approximate and exact solutions to the diffusion problem (Gerke and van Genuchten, 1993) and G_f is a geometry factor (set internally to 3 for a rectangular slab geometry). Water flow can occur in the reverse direction if the micropores are saturated. Here any excess water is instantaneously transferred to the macropores.

Solute transport in the micropores is calculated using the convection-dispersion equation with source-sink terms (kg $m^{-3}\ s^{-1}$) representing mass exchange between flow domains, U_e, crop uptake, U_c, degradation, U_d, losses to field drains, U_s, and losses due to regional groundwater flow, U_g:

$$\frac{\partial\left(c_{mic}\theta_{mic}+\left(1-f\right)\rho s\right)}{\partial t} = \frac{\partial}{\partial z}\left(D\,\theta_{mic}\,\frac{\partial c_{mic}}{\partial z} - qc_{mic}\right) - U_c - U_d - U_s - U_g \pm U_e \qquad [4]$$

where c_{mic} (kg m^{-3}) is the solute concentration in the liquid phase, s (kg m^{-3}) is the sorbed concentration in the solid phase, f (-) is the mass fraction of the solid material in contact with water in the macropore domain, ρ (kg m^{-3}) is the soil bulk density, θ_{mic} ($m^3\ m^{-3}$) is the micropore water content, accounting for an inaccessible soil volume due to anion exclusion, q (m s^{-1}) is the water flow rate, and D ($m^2\ s^{-1}$) is the dispersion coefficient, calculated as the sum of an effective diffusion coefficient and a dispersion term. Solute transport in the macropores is assumed to be dominated by convection.

The mass transfer term, U_e, accounts for both diffusion and convective flow:

$$U_e = \left(\frac{3\,D_e\,\theta}{d^2}\right)\left(c_{mac} - c_{mic}\right) + S_w c' \qquad [5]$$

where D_e ($m^2\ s^{-1}$) is an effective diffusion coefficient, c_{mac} (kg m^{-3}) is the solute concentration in the liquid phase in macropores, and c' (kg m^{-3}) indicates either the solute concentration in macropores or in 'accessible water' in the micropores, depending on the direction of water flow, S_w. The solute concentration in the water routed into the macropores at the soil surface is calculated assuming instantaneous equilibrium in a thin surface layer or mixing depth, z_{mix} (m).

Pesticide degradation, U_d, follows first-order kinetics and is in this study assumed to proceed at the same rate in both liquid and solid phases in both flow domains. The degradation rate coefficient, μ (s^{-1}), is adjusted for soil temperature by a modified form of the Arrhenius equation (Boesten and van der Linden, 1991) and soil moisture by a modified form of Walker's function (Walker, 1974). Equilibrium sorption partitioning is calculated using the Freundlich isotherm.

Solute loss to field drainage systems, U_s, is calculated assuming complete lateral mixing of solutes within a flow domain for each soil layer. Solute lost in lateral shallow groundwater flow, U_g, is calculated for each saturated soil layer using a retention time concept (Larsbo and Jarvis, 2003).

Calibration

The generalized uncertainty estimation (GLUE) framework deals with model parameter and prediction uncertainty within the context of Monte Carlo analysis (Beven and Binley, 1992). Usually, many parameter sets may equally well describe the observations according to some goodness-of-fit measure (goal function). Within the GLUE framework this is referred to as ‘equifinality’. If we accept this, it is not meaningful to search for unique parameter values. Therefore, the GLUE procedure is only concerned with evaluating the ‘likelihood’ of parameter sets as simulators of the observations. Likelihood is here used in a broad sense, meaning a specified measure of how well the outcome of a model and a parameter set describes the observations. Not all parameter sets will be acceptable simulators of the observations. GLUE does not provide any information about parameter interactions, but these are implicitly reflected in the likelihood values.

The outcome of GLUE will, to some extent, be dependent on a number of subjective choices. Prior parameter distributions should be based on all available information, which is often limited to expert judgement and past experience. Beven and Binley (1992) consider it unlikely that this choice will be critical since new observations are supposed to dominate the posterior distribution. They suggest using a uniform prior distribution when information is lacking. The choice of objective function should reflect the available observations and the purpose for which the modelling is required. Finally, a threshold defining acceptable parameter sets needs to be defined. Ideally the threshold should be chosen so that the variation in the measured data is covered by the simulations resulting from the accepted parameter sets. However, in many cases this may not be meaningful since both measurements and driving data for the simulations may be subject to error. All non-acceptable parameter sets are discarded by assigning them zero weight.

Even though GLUE was designed to identify acceptable parameter sets, information on individual parameters can be obtained from cumulative posterior parameter distributions (Beven and Freer, 2001). These distributions give information on the degree of parameter conditioning. Parameters with distributions differing the most from the prior distributions have been most conditioned by the process. Statistical measures, for example percentiles, can be calculated from the posterior parameter distributions and from model outputs in predictive simulations. These statistical measures are not absolute and can only be used for comparative purposes.

The simulation results are compared to measured data by some measure of goodness-of-fit, referred to as a goal function. We used the model efficiency (EF) (Loague and Green, 1991) since it is independent of differences in absolute values and units of observations in different data sets. In the case of multiple data sets (e.g. drainage rates and leaching rates), the goal function has to be formulated as a multi-objective function, in our case the overall model efficiency:

$$EF_{tot} = \sum_{i=1}^{m} w_i \frac{\sum_{j=1}^{n}\left(O_{ij} - \overline{O}_i\right)^2 - \sum_{j=1}^{n}\left(O_{ij} - P_{ij}\right)^2}{\sum_{j=1}^{n}\left(O_{ij} - \overline{O}_i\right)^2} \qquad [6]$$

where w_i is the weight given to each data set, m is the number of s, n is the number of observations in each group, O_{ij} and P_{ij} are the observed and simulated values, and $\overline{O}$ is the average of the observations for each group. If all observed and simulated values are identical, EF will be equal to one, while a negative value indicates a poor fit, meaning that the average value of the observations would be a better estimator than the model simulations.

Model application

Parameterisation

Since the harrowed layer of the *C* plot differed from the underlying soil, we divided the simulated profile into two horizons. This was done for both the *C* and *NT* microlysimeters (even though there were no clear horizons in the *NT* soil) to ensure that any differences in optimised parameters will be due to differences between treatments and not to differences in calibration techniques. The data from the microlysimeter experiments, using equal weights for drainage and leaching, were used in a GLUE analysis to optimise five parameters (Table 5) in the MACRO model governing macropore flow and transport. The diffusion pathlength, d, determines the exchange of water and solutes between pore domains (Eq. 3 and 5) and is a surrogate parameter for soil structure. The kinematic exponent, n^*, is hypothesised to be important for the possibilities to simulate differences in the tortuosity and connectivity of macropore systems between *C* and *NT*. The parameters included in the Monte Carlo analysis have been shown to be among the most sensitive for a similar experimental setup (Larsbo and Jarvis, 2005). Since the boundary water content, θ_{mic}, is not included in the calibration, varying θ_{sat} is equivalent to varying the macroporosity. Preliminary simulations suggested that optimised values for the two horizons for parameters $n^*$and θ_{sat} were positively correlated. To limit the computational work these parameters were assumed to be equal in both horizons. Initial water contents were included in the Monte Carlo analysis since these were not measured and likely varied between sampling occasions. Initial uncertainty intervals (Table 5) were based on measurements and previous experience with the model. We used uniform initial distributions for all parameters for the sake of simplicity and because our data did not support more advanced initial distributions. All other parameters (Table 6) except the irrigation rate were kept constant and assumed equal in both horizons for all microlysimeters, which is in accordance with the small differences between *C* and *NT* for the water retention (Table A1.1 and A1.2) and particle size distribution (Table 3) measurements. The average infiltration rate measured by tension infiltrometer at the pressure head –10 cm was used as K_b. In order to derive a value for K_{sat}, logarithms of the measured infiltration rates at –1 and –3 cm pressure head were extrapolated to zero pressure and then averaged (Messing and Jarvis, 1993). We generated 25000 parameter sets using Latin hypercube sampling. The same parameter sets were used to simulate all microlysimeters. Since the irrigation rates differed between microlysimeters (Table 2) each microlysimeter had to be simulated separately. We arbitrarily defined the 20 parameter sets with the largest EF_{tot} values for each microlysimeter as 'accepted' parameter sets.

Table 5. Parameters included in the GLUE analysis of the microlysimeter data and initial parameter uncertainty intervals.

Parameter	Initial uncertainty interval
Diffusion pathlength 0–6 cm (d_{top}), mm	1–70
Diffusion pathlength 6–18 cm (d_{sub}), mm	1–70
Kinematic exponent, macropores 0–18 cm (n^*), -	2–8
Total saturated water content 0–18 cm (θ_{sat}), %	44.2–53.7
Initial water content 0–18 cm (θ_{ini}), %	33.7–43.7

Table 6. Parameters treated as equal constants for both horizons in the Monte Carlo simulations of the microlysimeter data.

Parameter	Parameter value	Source
Saturated micropore hydraulic conductivity	0.12 mm h^{-1}	Tension infiltrometer
Saturated total hydraulic conductivity	42.5 mm h^{-1}	Tension infiltrometer
Micro/macropore boundary pressure head	10 cm	Default
Mixing depth	1 mm	Default
Diffusion coefficient of Cl^- in free water	1.9×10^{-9} m^2 s^{-1}	Known
Dispersivity	30 mm	Default
Tortuosity micropores	0.5	Default
Saturated micropore water content	43.7%	RetC-fitted
Residual micropore water content	0.0%	RetC-fitted
Van Genuchten N	1.15	RetC-fitted
Van Genuchten α	0.0050 cm^{-1}	RetC-fitted

Scenario simulations

Scenario simulations were run to study the effects of different tillage systems on pesticide leaching. We ran two sets of scenario simulations. The first set taking the uncertainty in calibrated parameter values into account by using all accepted parameter sets from the GLUE analysis for each tillage treatment. In the second set of scenario simulations (deterministic simulations) we used the 50th percentile values of each parameter in the accepted sets as best parameter estimates. For both sets we used parameter values derived from measurements for the top 30 cm of the profile whenever possible. However, preliminary scenario simulations showed that the simulated drainage pattern was not typical for Lanna (Larsson and Jarvis, 1999). In order to get a more realistic drainage pattern we changed the van Genuchten α to 0.046 cm^{-1} in the topsoil, which is the value used in the pre-defined surface water scenario for Lanna (FOCUS, 2001). We used driving data and soil, site and crop values for the remaining parameters from the Lanna scenario (FOCUS D1) assuming spring-sown cereals. In this scenario, tile drains are installed at a 13.5 m spacing and 1 m depth. The simulation period was 1 January 1976 to 30 April 1983. All simulations were run for two contrasting pesticides, one weakly sorbed and easily degraded referred to as *compound 1* (FOCUS dummy surface water compound 1) and one strongly sorbed and slowly degraded, referred to as *compound 7* (FOCUS dummy surface water compound 7). Even though the organic carbon content is of major importance for sorption, measured differences in organic carbon content were not accounted for in the scenario simulations since this would obscure the effects of using different parameter sets describing hydraulic properties in *C* and *NT*. The pesticides were applied at a dose of 1 kg ha^{-1} annually, with the date of application in each year determined using the PAT calculator (FOCUS, 2001), accounting for precipitation during a pre-defined application window between 1 May and 30 May. The complete parameterisation is presented in Table A2.1-A2.3.

The bottom boundary condition was chosen to allow simulation of a fluctuating water table in the soil profile. If the base of the profile is saturated, a no-flow condition is applied, which allows the water table to rise. When the soil dries out and the bottom layer in the profile becomes unsaturated, a zero potential condition is applied, which causes water to flow upwards into the profile.

According to FOCUS guidelines (FOCUS, 2001) we used only the last 16 months as assessment period. For this period, pesticides were applied on 4 May 1982. For the GLUE scenario simulations the target outputs were daily values of drainage rate and pesticide concentration in drain flow. We used the minimum, maximum and 50th percentile value of each output generated from the combined accepted parameter sets for the two treatments. The 50th percentiles were calculated using equal weights for the data sets (i.e. differences in EF_{tot} were neglected). For the deterministic simulations the outputs were hourly values of drainage rate and pesticide concentration in drain flow.

Results and discussion

GLUE microlysimeter simulations

Table 7 shows the EF values for the best simulation for each microlysimeter. MACRO 5.1 could fairly well simulate the measured data, with two *C* and four *NT* microlysimeters resulting in EF_{tot} values larger than 0.5. Two *C* and three *NT* microlysimeters resulted in negative EF_{tot} values and were therefore not included in further analysis. Leaching was generally better reproduced than percolation for both treatments probably because solute transport is more sensitive, compared to water flow, to the parameters included in the calibration. Examples of comparisons between measured and simulated percolation and leaching are presented in fig. 4 for *C* and fig. 5 for *NT*. The microlysimeters differ both in absolute values and in the dynamics for both percolation and leaching, with the *NT* microlysimeter showing a greater degree of preferential flow behaviour. For these examples, with EF_{tot} values of 0.31 and 0.75, the patterns of percolation and leaching are fairly well captured. This shows that the parameters and parameter intervals (Table 5) chosen for the Monte Carlo simulations give enough flexibility to model the measured data. Peak values tend to fall outside the prediction interval defined by the minimum and maximum values of the outputs generated from the accepted parameter sets. This suggests that the threshold for acceptable parameter sets may have been too restrictive.

In order to analyse differences between *C* and *NT* all accepted parameter sets for each treatment were combined into one group consisting of 120 parameter sets for *C* and another group of 120 for *NT*. Parameter distributions within the two groups could then be analysed statistically.

Table 7. Model efficiencies for the best GLUE simulation for each microlysimeter.

	EF conventional tillage				EF no tillage			
	Nr	Percolation	Leaching	Tot	Nr	Percolation	Leaching	Tot
Pre-	13	0.21	0.48	0.31	17	0.72	0.94	0.71
spring	14	0.36	0.50	0.37	18	0.88	0.69	0.75
sowing	15	-0.26	0.63	-0.08	19	0.22	0.59	0.13
	16	0.20	0.85	0.31	20	0.99	0.94	0.96
Mid	1	0.39	0.87	0.59	5	-0.16	0.70	0.02
growing	2	-	-	-	6	-0.18	-0.63	-0.52
season	3	0.79	0.80	0.77	7	0.07	0.62	0.26
	4	0.21	0.73	0.42	8	-	-	-
Pre-	21	-	-	-	25			
harvest						-0.35	0.44	-0.26
	22	-0.39	0.53	-0.12	26	0.50	0.80	0.53
	23	-	-	-	27	-0.18	0.35	-0.18
	24	-	-	-	28	-	-	-
Average		0.19	0.67	0.32		0.25	0.54	0.24

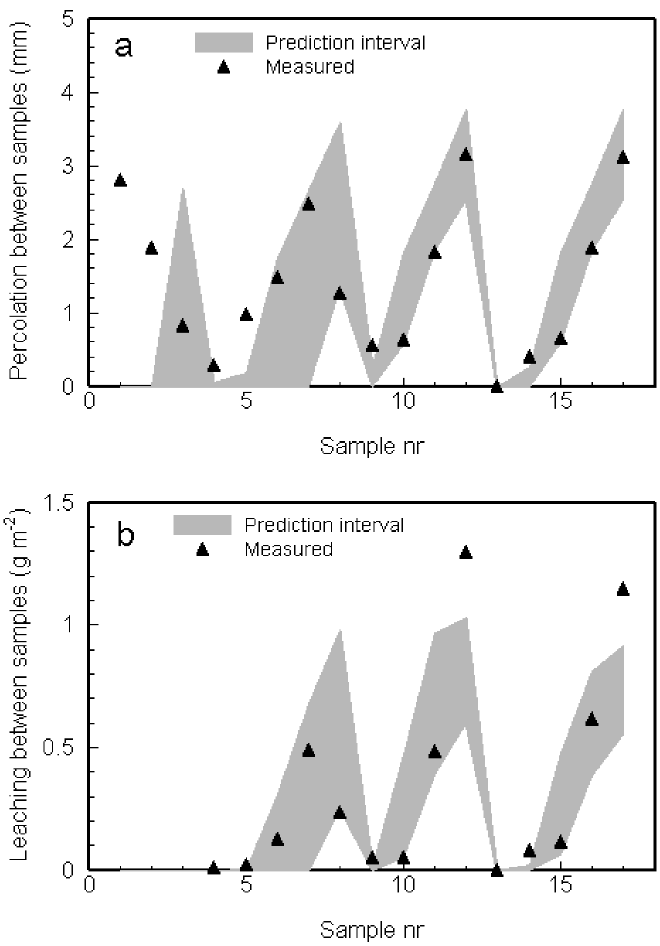

Fig. 4. Comparison between measured and simulated values for a conventional tillage microlysimeter (nr 16), a) percolation between measurements, and b) leaching amount between measurements. The prediction interval is defined by the minimum and maximum of the outputs from the accepted parameter sets.

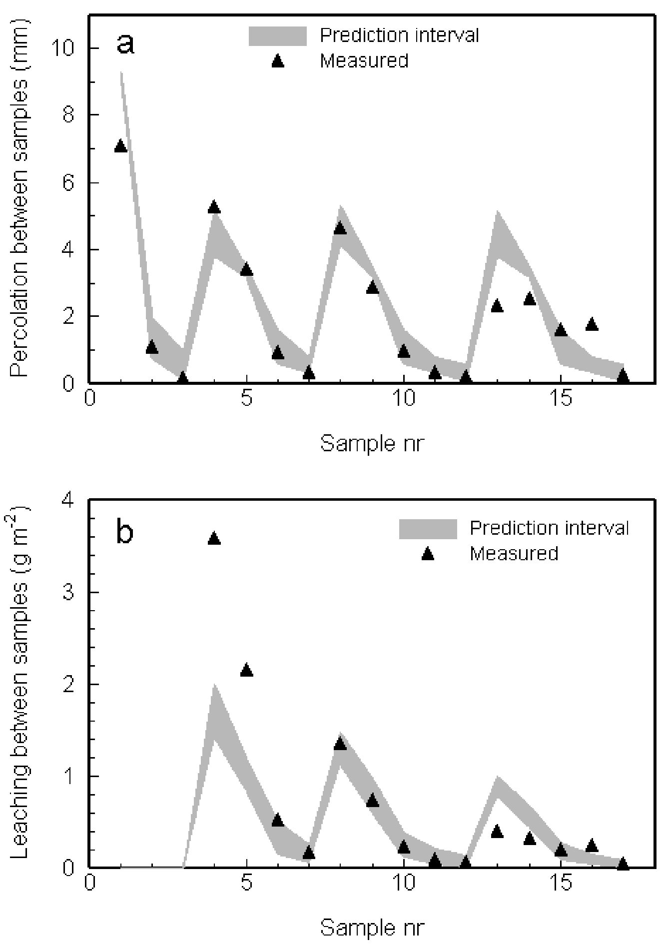

Fig. 5. Comparison between measured and simulated values for a no tillage microlysimeter (nr 18), a) percolation between measurements, and b) leaching amount between measurements. The prediction interval is defined by the minimum and maximum of the outputs from the accepted parameter sets.

Calibration

The values of d_{top} were approximately log-normally distributed with significantly different ($p=0.001$) means of the log-transformed values for *C* and *NT* using a t-test assuming unequal variances. Remaining parameter value distributions could not satisfactorily be transformed to normality. Hence, we could not test for differences between treatments for those parameters. Normalised histograms of the parameter distributions for d_{top} are presented in fig. 6 for both *C* and *NT*. A much larger proportion of the *C* simulations have values between 1 and 3 mm compared to *NT*, which indicates that the finer surface structure created by harrowing is reflected in the accepted parameter sets. It should also be noted that ca. 75% of the *NT* simulations have d_{top} values smaller than 15 mm. For d_{sub} the smallest value included in the group of parameter sets was 8.5 mm for *C* and 5.8 mm for *NT* (Table 8). This means that a certain degree of macropore flow in the 6–18 cm horizon was needed to simulate the experiments well for both treatments. This can also clearly be seen in the examples of dotty plots (fig. 7), which are typical for the treatments. For d_{sub}, all simulations with small parameter values have relatively small EF_{tot} values. If all simulations with large

EF_{tot} values are located in a limited area of the parameter interval it means that the parameter has been conditioned by the data and the parameter value is well defined. The values of θ_{sat} were always located in a well-defined interval for each microlysimeter (Table 8, fig. 7). The total saturated water content had large values for the *C pre-spring sowing* microlysimeters, corresponding well to the large values of macroporosity measured in the small cylinders sampled at the same time. Analyses of all other microlysimeters resulted in smaller values for the macroporosity except for one *C mid growing season* and one *NT pre-spring sowing* microlysimeter. Small values of θ_{sat} lead to high water flow velocity in the macropores and hence a fast breakthrough of water and solutes. The macropore tortuosity factor generally tended towards large values for the *C* treatment whereas it was poorly defined for *NT* (Table 8). Initial water contents were generally well defined for individual microlysimeters but parameter values differed within treatments. The poorly defined parameter values within each treatment are due to spatial variability in the field, measurement errors, parameter correlation, model errors and errors in parameter values not included in the calibration.

The best parameter estimates defined as the 50th percentile values from the groups of accepted parameter sets differ mainly for d_{top} and θ_{sat} (Table 9).

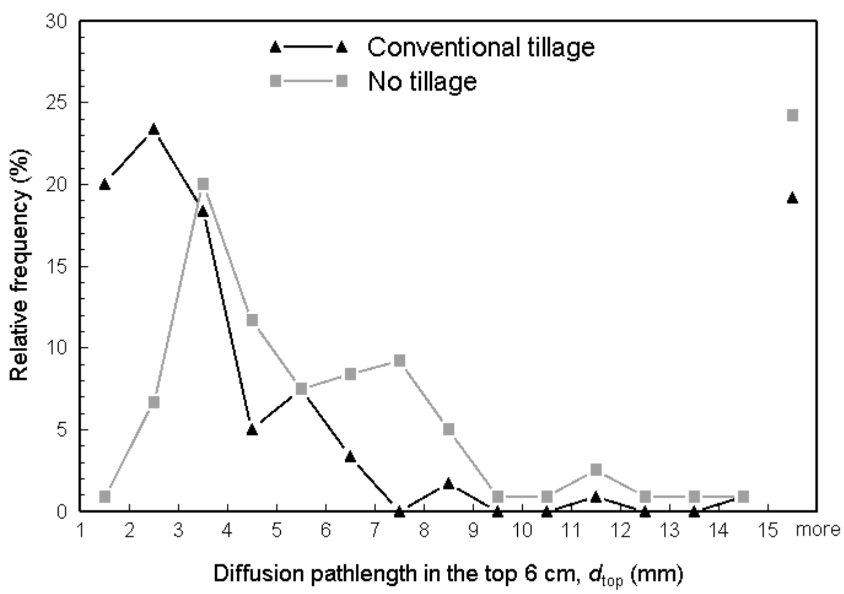

Fig. 6. Relative frequency of diffusion pathlength values in the top 6 cm for the groups of parameter sets

Table 8. Parameter intervals for the top twenty simulations for each microlysimeter. Only microlysimeters with twenty or more simulations with positive EFs are included.

	Conventional tillage Parameter†						No tillage Parameter†					
	Nr	d_{top}	d_{sub}	n^*	θ_{sat}	θ_{ini}	Nr	d_{top}	d_{sub}	n^*	θ_{sat}	θ_{ini}
Pre-	13	1.4–30	15–62	6.0–8.0	52.4–53.7	34.8–40.5	17	6.0–70	20–70	2.2–7.5	46.9–48.9	43.0–43.7
spring	14	1.3–6.8	22–69	6.0–8.0	52.5–53.7	34.8–43.6	18	2.4–5.1	23–67	2.2–7.8	44.9–46.7	40.6–42.7
sowing	15	-	-	-	-	-	19	3.7–60	15–69	2.2–3.5	50.2–52.1	40.1–43.6
	16	1.0–3.9	17–68	3.9–7.9	50.8–53.1	38.2–41.8	20	4.4–8.8	19–69	2.5–7.8	44.8–46.5	40.7–42.9
Mid	1	6.8–69	31–67	6.0–8.0	52.9–53.7	38.7–42.9	5	-	-	-	-	-
growing	2	-	-	-	-	-	6	-	-	-	-	-
season	3	2.4–5.6	37–69	2.2–7.5	45.0–46.7	38.9–41.4	7	2.7–7.7	21–66	5.4–8.0	45.7-47.4	37.9–41.5
	4	1.8–6.0	14–61	3.2–7.9	45.0–46.5	34.1–36.2	8	-	-	-	-	-
Pre-	21	-	-	-	-	-	25	-	-	-	-	-
harvest	22	-	-	-	-	-	26	1.3–62	5.8–68	2.3–5.3	47.4–49.4	34.0–36.6
	23	-	-	-	-	-	27	-	-	-	-	-
	24	-	-	-	-	-	28	-	-	-	-	-

† The parameters are: d_{top} (mm), diffusion pathlength in top 6 cm; d_{sub} (mm), diffusion pathlength in 6-18 cm depth; n^* (-), tortuosity factor macropores; θ_{sat} (%), total saturated water content; θ_{ini} (%), initial water content.

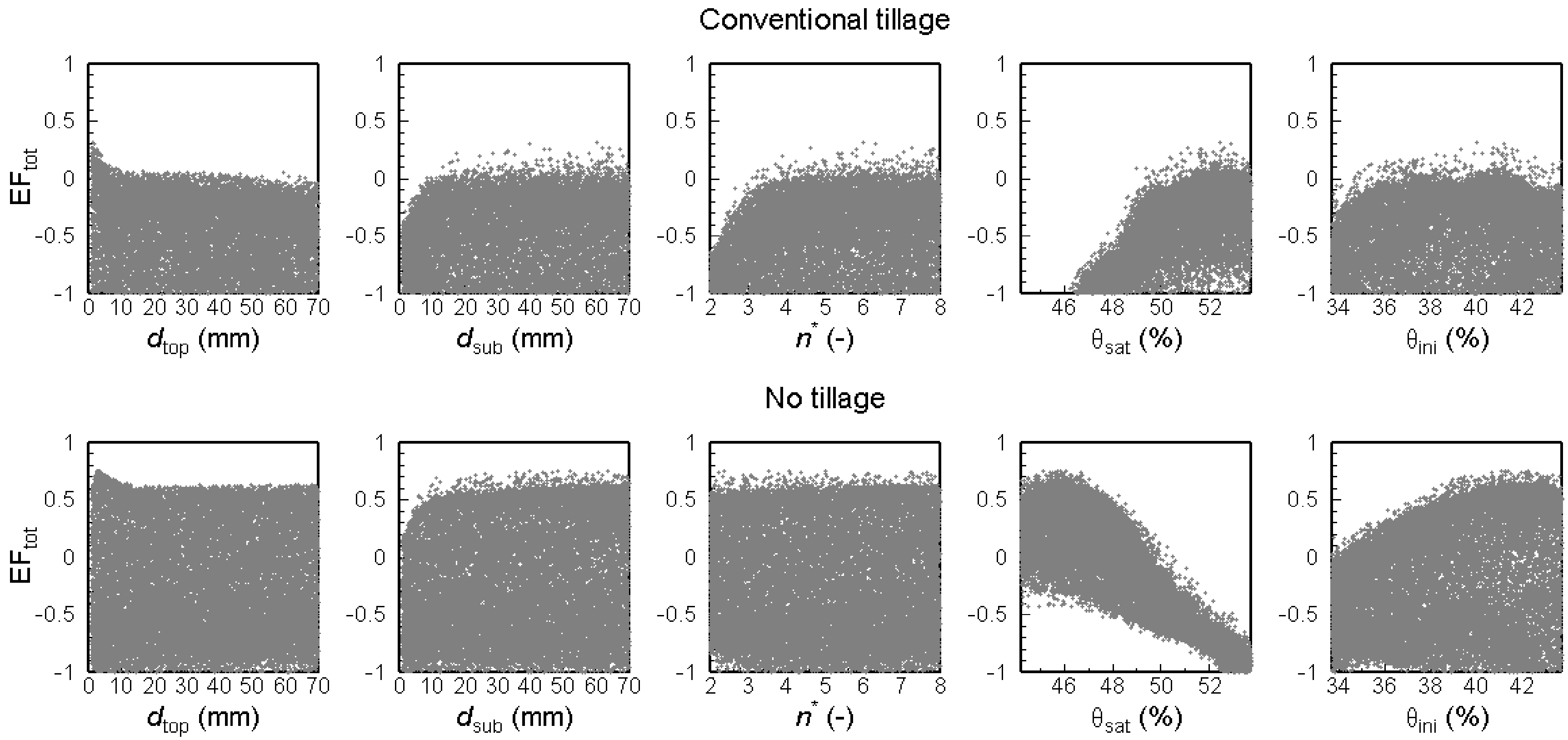

Fig. 7. Examples of dotty plots for all parameters included in the Monte Carlo analysis for conventional tillage and no tillage. Both examples are taken from the analysis of *pre-spring sowing* microlysimeters (nr 16 and 18). The parameters are: d_{top}, diffusion pathlength in top 6 cm; d_{sub}, diffusion pathlength in 6-18 cm depth; n^*, tortuosity factor macropores; θ_{sat}, total saturated water content; θ_{ini}, initial water content.

Table 9. Best estimate parameter values defined as the 50th percentile parameter values for the accepted groups of parameter sets for the two tillage treatments.

Parameter	Conventional tillage	No tillage
Diffusion pathlength 0–6 cm (d_{top}), mm	3.2	6.4
Diffusion pathlength 6–18 cm (d_{sub}), mm	48	52
Kinematic exponent, macropores 0–18 cm (n^*), -	7.1	4.7
Total saturated water content 0–18 cm (θ_{sat}), %	52.8	47.3
Initial water content 0–18 cm (θ_{ini}), %	39.3	41.8

Scenario simulations

The 50th percentiles of simulated drain flow rates for *C* and *NT* are shown in fig. 8. The differences between treatments were small and the uncertainty (not shown) was also small. This is probably because the overall water balance is not so sensitive to the parameters included in the calibration and drain response is dominated by the constant properties of the soil below the 30 cm depth. The treatment effects were much larger for pesticide concentrations in drainage water (fig. 9a and b). The 50th percentile values for *NT* were on average 3.4 times larger for *compound 1* and 4.6 times larger for *compound 7*. The large treatment effects reflect the trend of a faster solute breakthrough in the *NT* microlysimeter experiments, which was also reflected in the accepted parameter sets of d_{top} and θ_{sat}. The differences between treatments become more pronounced for the scenario simulations because pesticide transport is more sensitive to macropore structure than either water flow or non-reactive transport (Brown et al., 1999a, b). Although treatment effects were seemingly large, the uncertainty was huge and the 50th percentile values for *C* were always well inside the uncertainty intervals for *NT* and vice versa. The large variability in the scenario simulations reflects the large spatial variability and the sometimes poorly defined parameter values (Table 8).

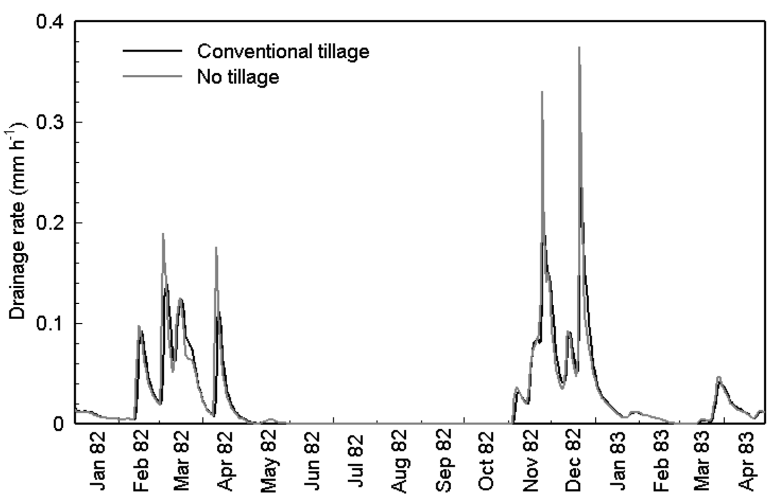

Fig 8. Fiftieths percentiles of drainage rates during the evaluation period of the GLUE scenario simulations.

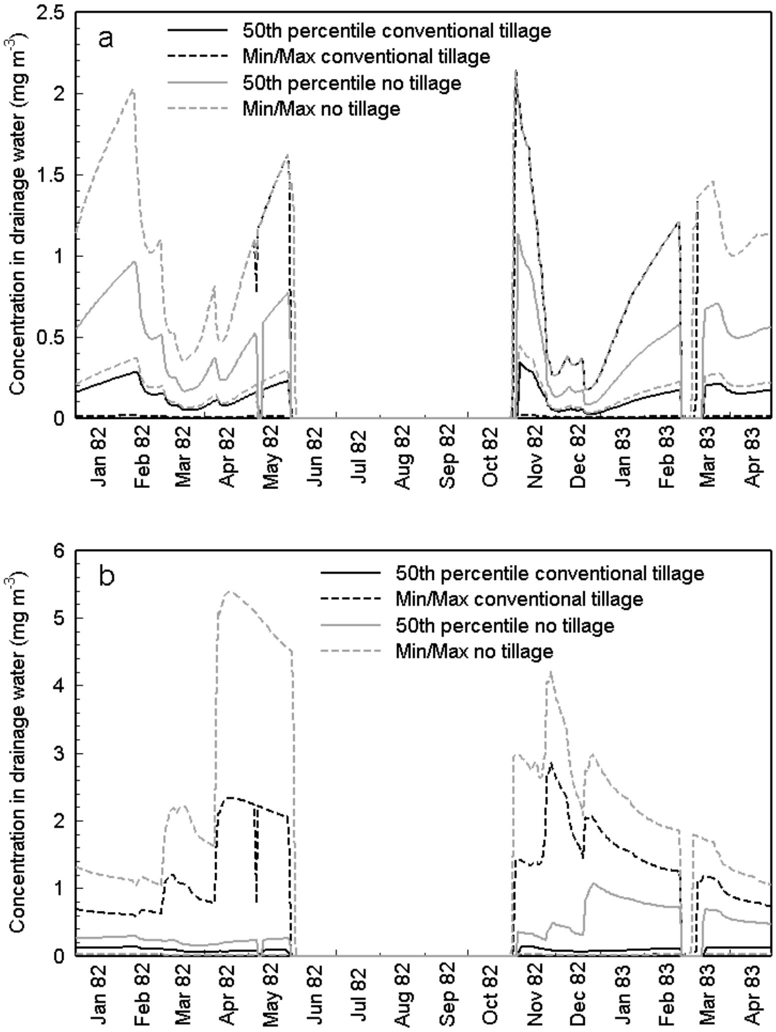

Fig 9. Daily values of concentration in drain flow during the evaluation period of the GLUE scenario simulations from the groups of accepted parameter sets, a) *compound 1* and b) *compound 7*.

The effects of the differences in best estimate parameter values (Table 9) are shown in fig. 10a and b, which show the results of the deterministic simulations. The maximum hourly concentrations in drain flow for *compound 1* were 0.32 and 1.1 mg m^{-3} for *C* and *NT* respectively. The corresponding values for *compound 7* were 0.09 and 1.1. The differences in drainage rates were again small (not shown).

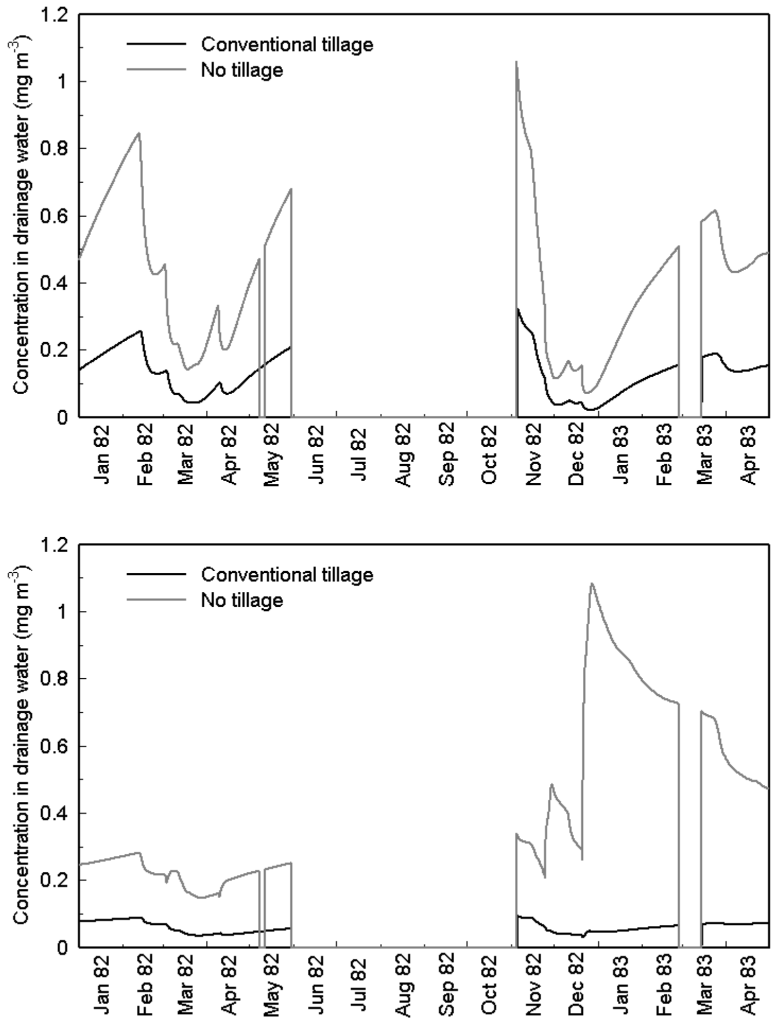

Fig 10. Hourly values of concentration in drain flow during the evaluation period of the deterministic scenario simulations, a) *compound 1* and b) *compound 7*.

FUTURE RESEARCH AND RECOMMENDATIONS

There are two reasons for the large uncertainty in parameter values and predictions for the two treatments. Firstly, the uncertainty in parameter values for each individual microlysimeter is often large. This uncertainty can possibly be reduced by more and better measurements to estimate the parameters not included in the calibration and to reduce the initial uncertainty intervals for calibrated parameters. Secondly, the large spatial variability within the *C* and *NT* treatments needs to be handled in a better way to reduce the uncertainty in predictions. One possible way to solve this problem is to use calibrated values for each microlysimeter in two-dimensional simulations instead of one parameter set for each treatment. The problem with such an approach is that the number of replicates needed to adequately represent the field might be very large.

CONCLUSIONS

The conclusions from the laboratory experiments are:

- The macroporosity was largest in the pre-spring sowing samples for conventional tillage, but otherwise temporal differences in soil hydraulic properties seemed small.
- Generally the no-till microlysimeters had a faster breakthrough of water and chloride.
- The variability in both the dynamics and in accumulated values of drainage and chloride leaching in the microlysimeter experiments is large.

The conclusions from the modelling exercise are:

- The observed differences in water flow and chloride leaching between treatments are reflected in the values for the parameter governing mass exchange between pore domains in the surface 6 cm of soil and in the macroporosity. Mass exchange is weaker and macroporosity is smaller in the no-till soil, both of which promote faster non-equilibrium macropore flow and transport.
- The differences in the scenario simulations between conventional tillage and no tillage are small with respect to drainage rates.
- For a weakly sorbed easily degraded compound and a strongly sorbed slowly degraded compound, the GLUE scenario simulations predict 3.4 and 4.6 times larger average concentrations in drainage water respectively for no-till compared with conventional tillage.
- The uncertainties in the concentrations in drainage water are large. This uncertainty reflects spatial variability in the field, errors in parameter values not included in the calibration, parameter correlations and model error.
- The maximum hourly concentrations in drainage water using best parameter estimates are 3.4 and 12 times larger for no-till compared with conventional tillage for a weakly sorbed easily degraded compound and a strongly sorbed slowly degraded compound.

REFERENCES

Bergström, L., N.J. Jarvis, and J. Stenström. 1994. Pesticide leaching data to validate simulation models for registration purposes. J. Environ. Sci. Health. (A) A29:1073-1104.

Beven, K., and A. Binley. 1992. The future of distributed models: Model calibration and uncertainty prediction. Hydrol. Process. 6:279-298.

Beven, K., and J. Freer. 2001. Equifinality, data assimilation, and uncertainty estimation in mechanistic modelling of complex environmental systems using the GLUE methodology. J. Hydrol. 249:11-29.

Boesten, J.J.T.I., and A.M.A. van der Linden. 1991. Modeling the influence of sorption and transformation on pesticide leaching and persistence. J. Environ. Qual. 20:425-435.

Brown, C.D., V.L. Marshall, A.D. Carter, A. Walker, D. Arnold, and R.L. Jones. 1999a. Investigation into the effect of tillage on solute movement to drains through a heavy clay soil. I. Lysimeter experiment. Soil Use Manage. 15:84-93.

Brown, C.D., V.L. Marshall, A. Deas, A.D. Carter, D. Arnold, and R.L. Jones. 1999b. Investigation into the effect of tillage on solute movement to drains through a heavy clay soil. II. Interpretation using a radio-scanning technique, dye-tracing and modelling. Soil Use Manage. 15:94-100.

Dunn, G.H., and Philips, R.E. 1991. Macroporosity of a well-drained soil under no-till and conventional tillage, Soil Sci. Soc. Am. J. 55:817-823.

Edwards, W.M., L.D. Norton, and C.E. Redmond. 1988. Characterizing macropores that affect infiltration into nontilled soil. Soil Sci. Soc. Am. J. 52:483-487.

Elliot, J.A., A.J. Cessna, W. Nicholaichuk, and L.C. Tollefson. 2000. Leaching rates and preferential flow of selected herbicides through tilled and untilled soil. J. Environ. Qual. 29:1650-1656.

FOCUS. 2001. FOCUS (Forum for the Coordination of Pesticide Fate Models and Their Use) surface water scenarios in the EU evaluation process under 91/414/EEC. Report of the FOCUS Working Group on Surface Water Scenarios. EC Document Reference Sanco/4802/2001-rev.1.221. EU Commission, Brussels.

Gaynor, J.D., D.C. MacTavish, and W.I. Findlay. 1995. Atrazine and metolachlor loss in surface and subsurface runoff from three tillage treatments in corn. J. Environ. Qual. 24:246-256.

Gerke, H.H., and M.T. van Genuchten. 1993. Evaluation of a first-order water transfer term for variably saturated dual-porosity flow models. Water Resour. Res. 29:1225-1238.

Germann, P.F. 1985. Kinematic wave approach to infiltration and drainage into and from soil macropores. Trans. ASAE 28:745-749.

Gish, T.J., A. Shirmohammadi, R. Vyravipillai, and B.J. Weinhold. 1995. Herbicide leaching under tilled and no-tillage fields. Soil Sci. Soc. Am. J. 59:895-901.

Heard, J.R., E.J. Kladivko, and J.V. Mannering. 1988. Soil macroporosity, hydraulic conductivity and air permeability of silty soils under long-term conservation tillage in Indiana. Soil Tillage Res. 11:1-18.

Isensee, A.R., R.G. Nash, and C.S. Helling. 1990. Effect of conventional vs. no tillage on pesticide leaching to shallow groundwater. J. Environ. Qual. 19:434-440.

Larsbo, M. and N. Jarvis. 2003. MACRO 5.0. A model of water flow and solute transport in macroporous soil. Technical description. Emergo 2003:6, Swedish Univ. of Agric. Sci, Dep. of Soil Sci., Uppsala.

Larsbo, M., S. Roulier, F. Stenemo, R. Kasteel, and N. Jarvis. 2005. An improved dual-permeability model of water flow and solute transport in the vadose zone. Vadose Zone J. 4:398-406.

Larsbo, M., and Jarvis, N. 2006. Information content of measurements from tracer microlysimeter experiments designed for parameter identification in dual-permeability models. J. Hydrol. 325:273-287.

Larsson, M.H., and N.J. Jarvis. 1999. Evaluation of a dual-porosity model to predict field-scale solute transport in a macroporous soil. J. Hydrol. 215:153-171.

Loague, K., and R.E. Green. 1991. Statistical and graphical methods for evaluating solute transport models: Overview and application. J. Contam. Hydrol. 7:51-73.

Mapa, R.B., Green, R.E., and Santo, L. 1986. Temporal variability in soil hydraulic properties with wetting and drying subsequent to tillage. Soil Sci. Soc. Am. J. 50:1133-1138.

Meek, B.D., W.R. DeTar, D. Rolph, E.R. Rechel, and L.M. Carter. 1990. Infiltration rate as affected by an alfalfa and no-till cotton cropping system. Soil Sci. Soc. Am. J. 54:505-508.

Messing, I., and N. Jarvis. 1993. Temporal variation in the hydraulic conductivity of a tilled clay soil as measured by tension infiltrometers. J. Soil Sci. 44:11-24.

Mualem, Y. 1976. A new model for predicting the hydraulic conductivity of unsaturated porous media. Water Resour. Res. 12:513-522.

Reynolds, W.D., and Zebchuk, W.D. 1996. Use of contact material in tension infiltrometer measurements. Soil Technol. 9:141-159.

Sadeghi, A.M., A.R. Isensee, and D.R. Shelton. 1998. Effect of tillage on herbicide dissipation: A side-by-side comparison using microplots. Soil Sci. 163:883-890.

van Genuchten, M.T. 1980. A closed-form equation for predicting the hydraulic conductivity of unsaturated soils. Soil Sci. Soc. Am. J. 44:892-898.

van Genuchten, M.T., F.J. Leij, and S.R. Yates. 1991. The RETC code for quantifying the hydraulic functions of unsaturated soils. EPA/600/2-91/065, US EPA, Office of Research and Development, Washington, DC.

Walker, A. 1974. A simulation model for prediction of herbicide persistence. J. Environ. Qual. 3:396-401.

ACKNOWLEDGEMENTS

The authors thank the staff at Lanna research farm and the Division of Soil Management at the Department of Soil Sciences, SLU for making the field plots available for this study.

Appendix 1. Water retention measurements

Table A1.1. Conventional tillage samples

		Pressure head								RetC-fitted parameters				
Sampling	porosity	-0.025	-0.2	-0.5	-1	-6	-50	-150	Macroporosity	θ_r	$\theta_{mic,sat}$	α	N	R^2
Pre-spring sowing	53.7	48.4	39.5	37.4	35.7	31.0	24.1	17.6	8.9	0.0	0.390	0.0061	1.16	0.983
	54.6	48.1	38.2	36.4	34.6	30.2	24.1	17.6	9.9	0.0	0.378	0.0064	1.15	0.979
	56.8	51.2	38.3	36.3	34.3	29.7	24.1	17.6	12.9	0.0	0.383	0.010	1.14	0.977
Early growing season	45.7	48.2	45.6	44.0	42.4	36.6	29.0	21.7	2.6	0.0	0.454	0.0052	1.15	0.987
	47.9	47.3	45.9	44.5	42.7	36.4	29.0	21.7	1.4	0.0	0.460	0.0063	1.15	0.988
	46.4	47.7	46.4	45.0	43.6	37.2	29.0	21.7	1.3	0.0	0.463	0.0049	1.16	0.990
Mid growing season	48.7	48.3	45.7	43.4	41.7	36.8	28.6	20.8	2.6	0.0	0.447	0.0040	1.17	0.981
	47.5	47.4	46.4	44.8	43.4	38.8	28.6	20.8	1.0	0.0	0.455	0.0022	1.21	0.991
	49.2	48.2	46.4	44.5	43.1	38.1	28.6	20.8	1.8	0.0	0.455	0.0028	1.19	0.988
Pre-harvest	44.6	46.1	44.1	42.6	41.0	36.4	32.5	24.6	2.0	0.0	0.439	0.0074	1.11	0.956
	43.7	46.8	44.0	42.6	41.3	37.1	32.5	24.6	2.8	0.0	0.434	0.0038	1.12	0.960
	43.7	47.3	44.6	43.7	42.3	37.4	32.5	24.6	2.7	0.0	0.446	0.0040	1.13	0.970

Table A1.2. No tillage samples

		Pressure head								RetC-fitted parameters				
Sampling	porosity	-0.025	-0.2	-0.5	-1	-6	-50	-150	Macroporosity	θ_r	$\theta_{mic,sat}$	α	N	R^2
Pre-spring sowing	50.5	51.7	47.5	45.8	44.3	39.0	28.6	21.8	4.2	0.0	0.469	0.0032	1.19	0.994
	50.5	52.4	50.7	49.1	47.6	42.0	28.6	21.8	1.7	0.0	0.500	0.0025	1.22	0.997
	51.2	50.3	46	44.6	43.0	37.8	28.6	21.8	4.3	0.0	0.456	0.0036	1.17	0.993
Mid growing season	42.9	44.9	43.7	42.3	40.9	36.9	30.5	21.7	1.2	0.0	0.427	0.0019	1.18	0.969
	47.8	48.4	43.4	41.7	40.2	35.6	30.5	21.7	5.0	0.0	0.427	0.0038	1.14	0.958
	46.2	47.0	44.0	42.2	40.5	35.8	30.5	21.7	3.0	0.0	0.433	0.0045	1.14	0.960
Pre-harvest	48.6	49.9	43.4	41.7	39.9	35.2	30.8	22.7	6.5	0.0	0.432	0.0076	1.12	0.958
	47.4	49.7	44.2	41.9	40.4	35.8	30.8	22.7	5.5	0.0	0.436	0.0067	1.12	0.961
	47.4	48.5	43.0	40.6	39.2	34.8	30.8	22.7	5.5	0.0	0.426	0.0088	1.11	0.949

Appendix 2. Scenario parameters

Table A2.1. Soil and site parameters. All values are from Table C11 (FOCUS, 2001) except where indicated.

Description	Name	Unit			Value		
Depth		cm	0-6	6-30	30-60	60-100	100-175
Basic properties							
Clay content	-	%	47	47	56	61	66
Silt content	-	%	46	46	41	37	31
Sand content	-	%	7	7	3	2	3
Organic carbon content	-	%	2.0	2.0	0.8	0.3	0.2
Bulk density	GAMMA	g cm^{-3}	1.35	1.35	1.42	1.42	1.42
Hydraulic properties							
Saturated water content	TPORV	%	Cal.[1]	Cal.[1]	46	47	47
Water content at wilting point	WILT	%	26	26	29	31	33
Residual water content	RESID	%	0	0	0	0	0
Micro/macropore boundary water content	XMPOR	%	43.8[2]	43.8[2]	42	45	45
Micro/macropore boundary tension	CTEN	cm	10	10	10	10	10
Van Genuchten N	N	-	1.15[3]	1.15[3]	1.05	1.05	1.05
Van Genuchten α	ALPHA	cm^{-1}	0.046[4]	0.046[4]	0.013[4]	0.011[4]	0.009[4]
Tortuosity factor micropores	ZM	-	0.5	0.5	0.5	0.5	0.5
Tortuosity factor macropores	ZN	-	Cal.[1]	Cal.[1]	2	2	2
Effective diffusion pathlength	ASCALE	mm	Cal.[1]	Cal.[1]	100	300	300
Saturated hydraulic conductivity	KSATMIN	mm h^{-1}	42.5[2]	42.5[2]	50	30	20
Micro/macropore boundary hydraulic conductivity	KSM	mm h^{-1}	0.1	0.1	0.3	0.2	0.1
Field drainage							
Drainage depth	DRAINDEP	m	1.0				
Drain spacing	SPACE	m	13.5				
Transmission coefficient at bottom boundary	BGRAD	h^{-1}	0.0				
Solute transport							
Mixing depth	ZMIX	mm	1.0				
Dispersivity	DV	cm	1.0				

[1] Values from the Monte Carlo analysis of microlysimeter data
[2] Derived from new measurements
[3] RetC-fitted from new measurements
[4] From pedotransfer functions built into MACRO 5.1

Table A2.2. MACRO 5.1 crop parameters for spring-sown cereals used in the scenario simulations. Parameters adapted from Table C2 and C3 (FOCUS, 2001).

Description	Name	Value (unit)
Maximum leaf area index	LAIMAX	4 $m^2\ m^{-2}$
Green leaf area index at harvest	LAIHARV	2 $m^2\ m^{-2}$
Root distribution	RPIN	60 %
Maximum crop height	HMAX	0.8 m
Root adaptability factor	BETA	0.2
Leaf development factor, growth	CFORM	2.0
Leaf development factor, senescence	DFORM	0.3
Initial leaf area index	LAI initial	0.01 $m^2\ m^{-2}$
Initial crop height	Height initial	0.01 m
Initial root depth	Depth initial	0.01 m
Maximum interception capacity	CANCAP	2 mm
Maximum interception fraction for pesticide	ZALP	0.9
Ratio of evaporation of intercepted water to transpiration	ZALP	1.0
Radiation attenuation factor	ATTEN	0.6
Solar radiation that reduces stomatal conductance by 50%	RI50[1]	55 W m^{-2}
Vapour pressure deficit that reduces stomatal conductance by 50%	VPD50[1]	100 Pa
Minimum stomatal resistance	RSMIN	50 s m^{-1}
Day of crop emergence	IDSTART	125 j.d.
Day of intermediate crop development	ZDATEMIN	126 j.d.
Day of maximum leaf area index	IDMAX	219 j.d.
Harvest day	IHARV	252 j.d.

[1] New parameters in MACRO 5.1

Table A2.3. Compound and degradation properties. All properties are assumed constant with depth. Values are adapted from FOCUS (2001). *Compound 1* is FOCUS dummy compound 1 and *compound 7* is FOCUS dummy compound 7.

Description	Name	Unit	*Compound 1*	*Compound 7*
Organic carbon partitioning coefficient	KOC[1]	$cm^3\ g^{-1}$	15	500
Degradation rate coefficient in topsoil[2]	DEG	d^{-1}	0.116	0.0139
Freundlich exponent	FREUND	-	1	1
Crop uptake factor	FSTAR	-	0.5	0.5
Reference temperature for degradation	TREF	°C	20	20
Degradation temperature response	TRESP	$°C^{-1}$	0.079	0.079
Degradation moisture response	EXPB	-	0.7	0.7
Washoff coefficient	FEXT	mm^{-1}	0.05	0.05
Canopy degradation rate coefficient	CANDEG	d^{-1}	0.0693	0.0693
Diffusion coefficient in free water	DIFF	mm s^{-1}	5.0×10^{-10}	5.0×10^{-10}

[1] The MACRO parameter is ZKD which is KOC times the organic carbon content
[2] Degradation is assumed equal in all phases and pore domains. Degradation is reduced in the subsoil through multiplication by the factors 0.5 (30–60 cm depth), 0.3 (60–100 cm depth) and 0.0 (100–175 cm depth).